Quench of Hot-Electron Real Space Transfer by Electronic Screening

Chun-Ting Liu, *Member, IEEE,* Serge Luryi, *Fellow, IEEE,* Paul A. Garbinski, Alfred Y. Cho, *Fellow, IEEE,* and Deborah L. Sivco

***Abstract*—We report a study of the hot-electron real space transfer (RST) between two InGaAs layers separated by a 200-nm InAlAs barrier. The electron heating is generated by an electric field applied parallel to one of the layers, which represents a two-dimensional hot-electron emitter. We observe a strong suppression of the RST by an increased concentration n_s of the emitter electrons. With increasing n_s, the critical heating voltage, required to initiate the RST, increases. At a fixed heating voltage, a sudden quench of the RST is observed as n_s increases. Both phenomena are explained by an electronic screening effect which smoothens out the nonuniformity of the electric field in the emitter channel.**

I. Introduction

THE EFFECT of hot-electron real space transfer (RST) in multilayer semiconductor structures, has generated a great deal of interest, both for its inherent physics and the possibility of device applications [1], [2]. The RST physics is rather involved because the effect is sensitive to the details of the electron energy distribution at high energies. Device applications are attractive because adjustments of the electron distribution occur very rapidly, with subpicosecond delays. Perhaps the most important electronic device based on the RST principle is the charge injection transistor or CHINT [2]. In recent years, this device has been studied extensively, both as a microwave transistor and as a logic element [3]. The peculiar advantage of CHINT for logic applications results from the basic symmetry of the RST current with respect to the polarity of the heating field [4].

The CHINT devices studied in this work (Fig. 1) were fabricated following the same procedure as described in [5]. The lattice-matched heterostructure was grown by molecular beam epitaxy on a semi-insulating InP substrate. The channel was defined by a trench obtained with a highly selective wet chemical etch of the InGaAs cap layer. Its length L_{ch} varies from 0.5 to 5 μm, and there are devices with three different channel widths W = 25, 50, and 75 μm for every L_{ch}. After the etching, the trench exposes the emitter channel to a complete depletion by the surface potential. Channel electrons are induced upon

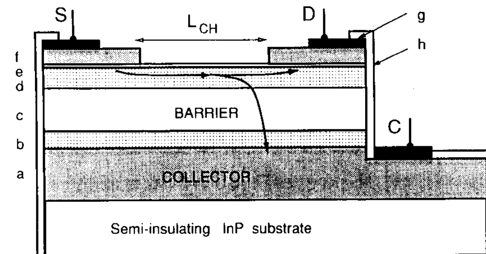

a: 5000 Å InGaAs n^+ (Si:10^{19})
b: 500 Å InGaAs n^- (Si:10^{17})
c: 2000 Å InAlAs u
d: 500 Å InGaAs n (Si:10^{16})
e: 25 Å InAlAs n^+ (Si:10^{19})
f: 200 Å InGaAs n^+ (Sn:10^{20})
g: 500 Å Ti / 1000 Å Au
h: Si_3N_4

Fig. 1. A cross section of the sample structure. The current from the emitter channel to the collector layer, as indicated by the downward arrow, arises from the real space transfer of hot electrons.

the application of a positive collector bias V_C, higher than a threshold value V_T, and their two-dimensional (2D) concentration n_s is controlled by the value of V_C relative to the source and by the barrier capacitance C.

The hot-electron RST occurs between the emitter and the collector InGaAs layers, which are separated by a 200-nm InAlAs barrier layer (the conduction-band discontinuity $\Phi_0 \approx 0.5$ eV). Electron heating is generated by a source-to-drain bias V_D. For small heating V_D, the thermionic transfer of emitter electrons over the barrier is insignificant. For high V_D, the heating electric field E along the 2D channel supplies energy to the emitter electrons at a rate higher than that of the electron energy loss to the lattice, and, in a steady state, the electron temperature T_e is higher than the lattice temperature T. As a consequence, the thermionic emission of hot electrons, which increases exponentially with T_e, becomes a dominant current path when V_D exceeds a critical value $V_D^{\rm crit}$. This increasing RST current gives rise to a negative differential resistance in the drain circuit.

We have investigated the hot-electron RST in a total of 27 samples with five different channel lengths L_{ch}. In particular, we focus on the dependence of RST on V_C, L_{ch}, and the lattice temperature T. As V_C increases, so does n_s, while the effective barrier height Φ for RST decreases [6]. Because of the reduction of barrier height, one could expect that an increase of V_C should reduce $V_D^{\rm crit}$. Contrary

Manuscript received January 18, 1991; revised April 16, 1991. The review of this paper was arranged by Associate Editor M. Shur.
C. T. Liu was with AT&T Bell Laboratories, Murray Hill, NJ 07974. He is now with AT&T Bell Laboratories, Allentown, PA 18103-1285.
S. Luryi, P. A. Garbinski, A. Y. Cho, and D. L. Sivco are with AT&T Bell Laboratories, Murray Hill, NJ 07974.
IEEE Log Number 9101555.

0018-9383/91/1100-2417$01.00 © 1991 IEEE

to this expectation, we observe a monotonic increase of $V_D^{\rm crit}$ as a function of increasing V_C. Moreover, when the RST current is measured at a fixed V_D, it first increases with V_C as Φ is decreasing, but then exhibits an abrupt drop at a critical $V_C^{\rm crit}$. The drop can be as large as 80%, indicating a quench of the RST current at $V_C^{\rm crit}$. Our data suggest that both the increase of $V_D^{\rm crit}$ with increasing V_C and the quench of the RST at $V_C^{\rm crit}$ can be explained by an electronic screening effect which smoothens out the nonuniformity of the channel electric field. This nonuniformity exists because of the gating effect on the channel by the highly conducting collector layer. The screening becomes more effective as in increasing V_C increases n_s.

The fact that the charge injection by RST is strongly nonuniform along the channel has been previously noted in several analytic models [6], [7] and Monte Carlo simulations [8], [9]. However, the important role of the electronic screening in the hot-electron RST has never been directly addressed. Experimentally, a quench behavior of the RST has been observed in a GaAs/AlGaAs CHINT device by Kastalsky *et al.* [10] who proposed a model based on the channel pinch-off effect. A similar behavior has also been reported in a InGaAs/InAlAs CHINT without explanations [4]. Our present study indicates that the quench effect occurs at much lower values of V_D than would be required for a pinch-off of the channel. We have developed a simple model, based on the gradual channel approximation, commonly used in the analysis of field-effect transistors [11]. The model qualitatively explains the observations and is consistent with our measurements made at T between 77 and 300 K.

II. Dependence of the RST on the Electron Concentration and the Channel Length

Fig. 2 shows the data taken at 300 K from a sample with $L_{\rm ch}$ = 5 μm and W = 75 μm. The drain current I_D and the collector current I_C are shown in Fig. 2(a) as a function of the heating voltage V_D at fixed values of V_C. The dependences $I_D(V_D)$ (solid curves) and $I_C(V_D)$ (dotted curves) are displayed for seven different values of V_C. As the heating V_D increases, I_C gradually rises as a result of the RST, and, consequently, I_D increases sublinearly with V_D. When V_D reaches $V_D^{\rm crit}$ (indicated by arrows), an abrupt drop of I_D occurs accompanied simultaneously with a sudden increase of I_C, indicating the onset of a large hot-electron RST current. As V_C increases from 0.5 to 3.5 V, a monotonic increase, instead of the expected decrease, of $V_D^{\rm crit}$ is clearly observed.

In Fig. 2(b) the drain current is shown as a function of V_C taken at a low heating voltage V_D = 0.05 V. At such a low V_D, there is practically no RST current, and I_C is due to a leakage from the emitter channel to the collector layer which at V_C = 4 V is approximately 0.6 mA at 300 K, and drops to ~4 μA at 77 K. (The temperature effect on the data will be discussed in connection with Fig. 4.) As seen from Fig. 2(b), for $V_C \gtrsim 0.5$ V, the drain current I_D increases linearly with V_C. Extrapolating the

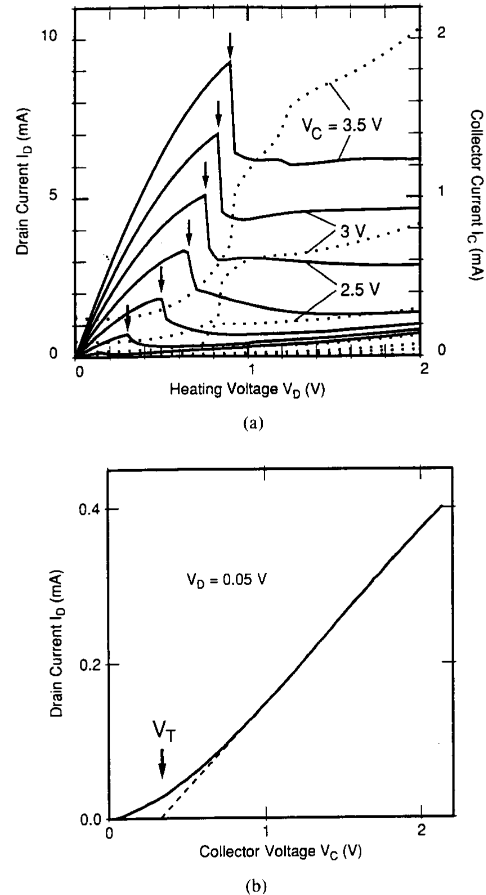

Fig. 2. Basic device characteristics at room temperature. $L_{\rm ch}$ = 5 μm, and W = 75 μm sample. (a) I_D (solid curves) and I_C (dotted curves) versus V_D at V_C = 3.5, 3, 2.5, 2, 1.5, 1, and 0.5 V (from the top downward). Arrows indicate the onset of the instability and the sudden increase of the RST current. (b) Drain current I_D versus V_C at V_D = 0.05 V. At this low V_D, there is no RST and V_C acts like the gate voltage of a field-effect transistor. The linear extrapolation to I_D = 0 gives V_T = 0.33 V for this sample.

linear region of I_D, we determine the threshold voltage V_T, which for this device turns out to be V_T = 0.3 V. For low V_D, the carrier concentration in the channel is uniform, $n_s(V_D = 0) = n_s(x = 0) \equiv n_0$, and n_0 increases linearly with V_C above the threshold: $n_0 = C(V_C - V_T)/e$. The observed linear $I_D(V_C)$ dependence indicates that the electron mobility μ does not appreciably vary with V_C.

At $V_D = V_D^{\rm crit}$, the gradual channel approximation gives the following estimate for the value of n_s at the drain end of the channel: $n_s(L_{\rm ch}) = C(V_C - V_T - V_D^{\rm crit})/e$, corresponding to ~$7.4 \times 10^{11}$ cm^{-2} for V_C = 3.5 V (from the thickness and the dielectric constant of the barrier layer $C/e \sim 3.4 \times 10^{11}$ cm$^{-2} \cdot$ V^{-1}). Therefore, the onset of the large RST cannot arise from a complete depletion of n_s at the drain end. From the values of n_s and I_D at $V_D^{\rm crit}$, we estimate the electron velocity at the drain end to be ~1.1×10^7 cm/s. Therefore, μ is still in the constant

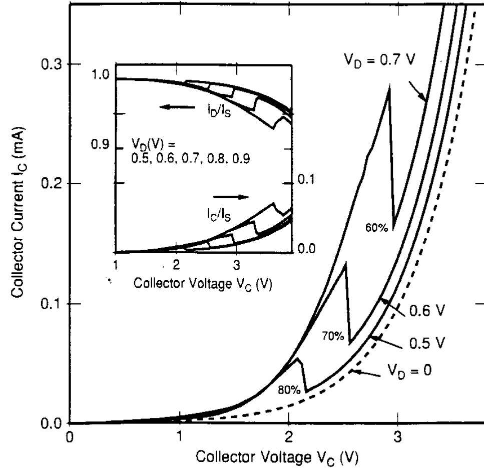

Fig. 3. Collector characteristics I_C versus V_C at a fixed heating voltage. $V_D = 0$ (dashed curve), 0.5, 0.6, and 0.7 V (solid curves). The difference between the solid curves and the dashed curve is the RST current. The percentages indicate the amount of the RST current drop at the critical point. Inset: collector-bias dependence of the ratios I_D/I_S and I_C/I_S for five different values of V_D.

range as a function of V_D [12]. It is also seen from Fig. 2(a) that at V_D^{crit} the average electric field along the channel, $V_D^{\text{crit}}/L_{\text{ch}}$, is only ~300 V/cm for $V_C = 0.5$ V and is ~1.8 kV/cm for $V_C = 3.5$ V. At such low fields, the population of satellite valleys in the conduction band is insignificant [13].

We see from Fig. 2(a) that $V_D^{\text{crit}} = 0.83$ V for $V_C = 3$ V, and it is 0.9 V for $V_C = 3.5$ V. If I_C is monitored with V_D fixed at 0.85 V while V_C is swept from 0.5 to 3.5 V, it will first increase with V_C for $V_C \leq 3$ V, but will exhibit a drop when V_C changes from 3 to 3.5 V. This observation is illustrated in Fig. 3 which plots I_C as a function of V_C for four different values of V_D. For $V_D = 0$ (dashed curve), I_C is the leakage current. For $V_D \neq 0$, the additional I_C from the leakage current is the RST current. The RST current first increases with V_C, as the effective Φ is lowered. At a critical value V_C^{crit}, however, I_C shows a sharp decrease which at $V_D = 0.5$ V is as large as 80%. This indicates that *the hot electron RST current is suddenly quenched* by the increasing V_C. After the quench point, the missing RST current is picked up at the drain electrode, resulting in a sharp surge of I_D, as shown in the inset of Fig. 3. The inset plots I_C/I_S and I_D/I_S as a function of V_C for five different values of V_D, where $I_S \equiv I_D + I_C$ is the total source current. The inset also shows that V_C^{crit} increases with V_D.

We have investigated 27 devices (from the same wafer) with five different values of L_{ch}. Fig. 4 summarizes our observations for V_D^{crit}. Fig. 4(a) shows V_D^{crit} as a function of $V_C - V_T$ for five different value of L_{ch}. For each sample, the threshold value V_T is determined in the same way as shown in Fig. 2(b). The data for $L_{\text{ch}} = 5$ μm correspond to those in Fig. 2(a). The following points are to be noted from the figure: 1) V_D^{crit} increases monotonically

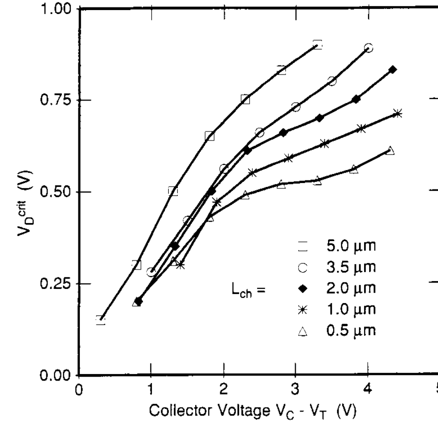

(a)

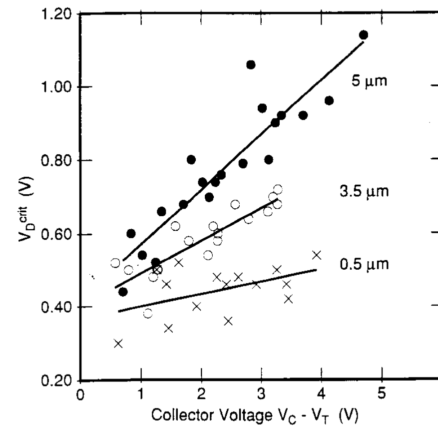

(b)

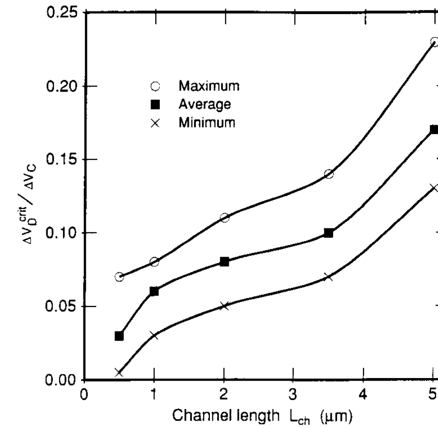

(c)

Fig. 4. The critical heating bias V_D^{crit} for the onset of the RST instability. (a) Dependence on $V_C - V_T$ for five individual samples with different channel length L_{ch}. (b) Dependence on $V_C - V_T$ representing a large number of devices with $L_{\text{ch}} = 5$ μ (●), 3.5 μm (○), and 0.5 μm (×). The straight lines represent the best linear fit to the data points for each L_{ch}. (c) Channel length dependence of $\Delta V_D^{\text{crit}}/\Delta V_C$. Circles and crosses are, respectively, from devics which give maximum and minimum $\Delta V_D^{\text{crit}}/\Delta V_C$. Blocks are the average values from all the investigated devices.

with $V_C - V_T$ for every L_{ch}; and 2) the slope $\Delta V_D^{crit}/\Delta V_C$ gradually decreases with increasing $V_C - V_T$. In Fig. 4(b), we plot V_D^{crit} versus $V_C - V_T$ obtained from a large number of samples with different L_{ch}. Each device is represented by several (3–5) points in the figure. The straight lines represent the best linear fit to the data points for each L_{ch}. The figure shows that: 3) the slope $\Delta V_D^{crit}/\Delta V_C$ increases with L_{ch}; and 4) at any given $V_C - V_T$, V_D^{crit} increases with L_{ch}. In Fig. 4(c), we plot $\Delta V_D^{crit}/\Delta V_C$ as a function of L_{ch}. Circles and crosses are, respectively, from samples which give maximum and minimum $\Delta V_D^{crit}/\Delta V_C$, and blocks are the average values form all the samples. The figure clearly shows that: 5) the slope $\Delta V_D^{crit}/\Delta V_C$ is nonvanishing for all the investigated samples and it increases with L_{ch}.

III. Influence of the Lattice Temperature

We have also studied the dependence of RST on the lattice temperature T between 77 and 300 K. Fig. 5(a) plots the $I_D(V_D)$ characteristics of a $L_{ch} = 2$ μm and $W = 50$ μm sample,for three different T, taken at three different valus of V_C. (The accompanying plot of I_C is omitted in order not to overburden the graph. Apart from the above-mentioned decrease of the leakage current, the behavior of I_C at lower temperatures is similar to that shown in Fig. 2(a), i.e., a sudden increase of I_C occurs simultaneously with the abrupt drop in I_D.) As seen from Fig. 5(a), at a fixed V_C, e.g., the solid curves for $V_C = 5$ V, the decreasing T leads to an increase in I_D at small V_D ($\lesssim 0.1$ V), resulting from an enhancement of the mobility μ at lower temperatures. The increasing I_D with decreasing T is accompanied by a decreasing V_D^{crit}. The unexpected increase of V_D^{crit} with increasing V_C is apparent for all three different T.

Fig. 5(b) summarizes V_D^{crit} as a function of V_C obtained for the same device at eight different temperatures. From this figure, we make an interesting observation that $\Delta V_D^{crit}/\Delta V_C$ is independent of T between 77 and 300 K.

Fig. 5(c) plots the temperature dependence of $(V_D^{crit})^2$ and $1/I_D$ taken at $V_D = 0.05$ V in a log-log scale for three different values of V_C. The figure clearly shows that both $(V_D^{crit})^2$ and $1/I_D$ follow exactly the same dependence on T. At $V_D = 0.05$ V, assuming that n_s is a constant, this dependence corresponds to $1/\mu(T)$. From this figure, we therefore conclude that the product $\mu \cdot (V_D^{crit})^2$ is independent of T. The T dependence of μ, resulting from the electron scattering by phonons, ionized impurities, and alloy fluctuations, is well understood [14].

IV. Model and Analysis

Both the increase of V_D^{crit} with increasing V_C and the quench of the hot-electron RST at V_C^{crit} can be explained by an electronic screening effect which smoothens out the nonuniform channel field $E(x)$. The total potential drop from the source to the drain is fixed by V_D, but $E(x)$ is also affected by the potential V_C of the collector layer,

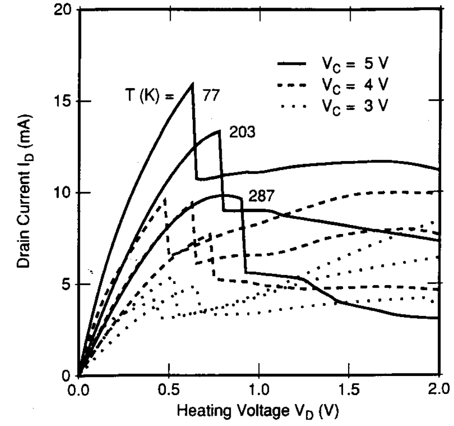

(a)

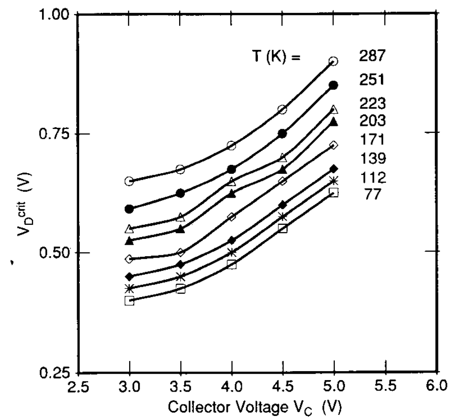

(b)

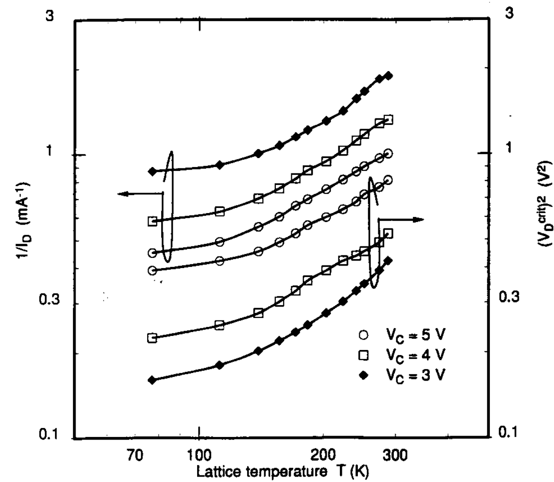

(c)

Fig. 5. Influence of the lattice temperature. $L_{ch} = 2$ μm, $W = 50$ μm. (a) $I_D(V_D)$ characteristics taken at three different T and V_C. (b) V_D^{crit} versus V_C for eight different T. (c) Log-log plot of $(V_D^{crit})^2$ and $1/I_D$ against T for three different V_C. The I_D value is measured at $V_D = 0.05$ V.

which is highly conducting and can be assumed to be an equipotential plate. In the presence of a current flow, the voltage drop along the channel leads to a lower carrier concentration near the drain. In the approximation of a constant mobility, this, in turn, requires an increasing lateral field $E(x)$, in order to maintain a constant channel current (neglecting the RST). This situation is well described by the gradual channel approximation [11]

$$n_s^2(x) = n_0^2 - \frac{I_D}{W}\frac{2C}{e^2\mu}x \tag{1}$$

$$E(x) = \frac{I_D}{Wen_0\mu}\left(1 - \frac{I_D}{Wn_0^2}\frac{2C}{\mu e^2}x\right)^{-1/2}$$

$$\approx \frac{I_D}{Wen_0\mu}\left(1 + \frac{CI_D}{We^2n_0^2\mu}x\right). \tag{2}$$

At elevated T_e, the electronic system is nondegenerate, and the energy-balance equation can be written in the form

$$\frac{k(T_e - T)}{\tau_E} = e\mu E^2 \tag{3}$$

where τ_E is the electron energy relaxation time due to inelastic scattering. Thus in the constant μ approximation, $T_e(x) \propto E^2(x)$. Furthermore, because the RST current $J(x)$ is proportional to $\exp(-\Phi/kT_e)$, the local injection current density $J(x)$ is an exponentially strong function of $E(x)$. Since the total potential drop from the source to the drain is fixed by V_D, a larger nonuniformity of $E(x)$ results in a higher overall injection of hot electrons. Thus we can expect a smaller V_D^{crit} when the nonuniformity of $E(x)$ is higher. In our approximation, this effect is described by the second term in (2), which decreases with increasing n_0. Therefore, V_D^{crit} increases with $V_C - V_T$. This also explains why $\Delta V_D^{\text{crit}}/\Delta V_C$ decreases with increasing V_C. Finally, since at low biases I_D is proportional to V_D/L_{ch} and decreases with increasing L_{ch} for a given V_D, the increases of both V_D^{crit} and $\Delta V_D^{\text{crit}}/\Delta V_C$ with L_{ch} are also explained by (2).

Our model is consistent with the observed temperature effects. Because the electronic screening only depends on T_e but not on T, the lattice temperature has no effect on $\Delta V_D^{\text{crit}}/\Delta V_C$, as seen in Fig. 5(b). The observation that the product $\mu \cdot (V_D^{\text{crit}})^2$ is independent of T indicates that for $T_e >> T$ the critical steady-state energy input to the emitter electrons required for the onset of the sharp increase of the RST is not a function of T. The critical power input is thus completely determined by τ_E and the width of the hot-electron distribution function parameterized by T_e. This implies that the RST phenomenon can provide a unique tool for studying hot electron transport in multilayer semiconductor structures and modern electronic devices.

Finally, it should be pointed out that the model can be improved and made more quantitative by including effects on the channel from the real space transfer current itself. Such an analysis requires numerical modeling and will be published elsewhere.

References

[1] K. Hess, "Principles of hot electron thermionic emission (real space transfer) in semiconductor heterolayers and device applications," *Festkörperprobleme*, vol. 25, p. 321, 1985.

[2] S. Luryi, "Hot-electron transistors," in *High-Speed Semiconductor Devices*, S. M. Sze, Ed. New York, Wiley, 1990, ch. 7, pp. 399–461.

[3] ——, "Charge injection transistors and logic circuits," *Superlattices and Microstructures*, vol. 8, no. 4, 1990.

[4] S. Luryi, P. M. Mensz, M. R. Pinto, P. A. Garbinski, A. Y. Cho, and D. L. Sivco, "Charge injection logic," *Appl. Phys. Lett.*, vol. 57, pp. 1787–1789, 1990.

[5] P. M. Mensz, P. A. Garbinski, A. Y. Cho, D. L. Sivco, and S. Luryi, "High transconductance and large peak-to-valley ratio of negative differential conductance in three-terminal InGaAs/InAlAs real-space transfer devices," *Appl. Phys. Lett.*, vol. 57, pp. 2558–2560, 1990.

[6] A. A. Grinberg, A. Kastalsky, and S. Luryi, "Theory of hot electron injection in CHINT/NERFET devices," *IEEE Trans. Electron Devices*, vol. ED-34, pp. 409–419, 1987.

[7] S. Luryi and A. Kastalsky, "Hot electron injection devices," *Superlattices and Microstructures*, vol. 1, pp. 389–400, 1985.

[8] I. C. Kizilyalli and K. Hess, "Physics of real-space transfer transistors," *J. Appl. Phys.*, vol. 65, p. 2005, 1989.

[9] R. Sakamoto, K. Akai, and M. Inoue, "Real-space transfer and hot-electron transport properties in III-V semiconductor structures," *IEEE Trans. Electron Devices*, vol. 36, p. 2344, 1989.

[10] A. Kastalsky, M. Milshtein, L. G. Shantharama, J. Harbison, and L. Florez, "New features of real-space hot-electron transfer in the NERFET," *Solid-State Electron.*, vol. 32, pp. 1841–1844, 1989.

[11] See, for example, S. M. Sze, *Physics of Semiconductor Devices*, 2nd ed. New York: Wiley-Interscience, 1981.

[12] E. Kobayashi, C. Hamaguchi, T. Matsuoka, and K. Taniguchi, "Monte Carlo study of hot-electron transport in an InGaAs/InAlAs single heterostructure," *IEEE Trans. Electron Devices*, vol. 36, p. 2353, 1989.

[13] R. R. Nag, S. R. Ahmed, and M. Deb Roy, "Electron velocity in short samples of $Ga_{0.47}In_{0.53}As$ at 300 K," *IEEE Trans. Electron Devices*, vol. ED-33, p. 788, 1986.

[14] J. R. Hayes, A. R. Adams, and P. D. Greene, "Low-field carrier mobility," in *GaInAsP Alloy Semiconductors*, T. P. Pearsall, Ed. New York: Wiley-Interscience, 1982, ch. 8, pp. 189–212.

*

Chun-Ting Liu (S'89–M'90) was born in Taiwan, Republic of China, on December 22, 1961. He received the B.S. degree from the National Taiwan University in 1983, and the M.S. and Ph.D. degrees from Princeton University, Princeton, NJ, in 1987 and 1990, respectively.

He joined the Optoelectronic Device Research Department of AT&T Bell Laboratories at Murray Hill, NJ, in 1990, and was subsequently transferred to the VHS SRAM Technology Development Group at Allentown, PA in 1991. He has published papers ranging from the optical and magnetotransport properties of nanometer surface superlattices to the hot-electron transport phenomena in short-channel devices, and invented a novel photovoltaic transistor.

Dr. Liu a member of the American Physical Society, the Materials Research Society, and the Photonic Society of Chinese Americans.

Serge Luryi (M'81-SM'85-F'89) received the M.Sc. and Ph.D. degrees in theoretical physics from the University of Toronto, Toronto, Ont., Canada, in 1975 and 1978, respectively.

Since 1980, he has been with AT&T Bell Laboratories, Murray Hill, NJ, where he is currently a Distinguished Member of Technical Staff in Compound Semiconductor Device Research Laboratory. His main research interests are in the physics of exploratory semiconductor devices.

*

Paul A. Garbinski, photograph and biography not available at the time of publication.

*

Alfred Y. Cho (S'57-M'60-SM'79-F'81) received the B.S., M.S., and Ph.D. degrees in electrical engineering from the University of Illinois in 1960, 1961, and 1968, respectively.

He is Director of the Materials Processing Research Laboratory at AT&T Bell Laboratories, Murray Hill, NJ. He joined Bell Laboratories in 1968 where he developed a crystal growth technology called molecular-beam epitaxy (MBE). His many significant research accomplishments include the construction of surface phase diagram for MBE crystal growth, the first fabrication of an MBE artificial superlattice, the first MBE IMPATT diode, mixer diode, and field-effect transistor operating at microwave frequencies, and the first MBE double-heterostructure laser operating CW at room temperature. His recent work is in the area of quantum-well devices. He has published over 250 papers in surface physics, crystal growth, and device physics and performance. He holds 43 patents on crystal growth and semiconductor devices related to MBE.

Dr. Cho is a recipient of the Electronics Division Award of the Electrochemical Society (1977), the American Physical Society International Prize for New Materials (1982), the IEEE Morris N. Liebmann Award (1982), the University of Illinois Electrical and Computer Engineering Distinguished Alumnus Award (1985), the Chinese Institute of Engineers USA Distinguished Achievement Award (1985), the GaAs Symposium Award-Ford (1986), the Heinrich Welker Medal-Siemens (1986), the Solid State Science and Technology Medal of the Electrochemical Society (1987), the College of Engineering Alumni Honor Award of the University of Illinois (1988), the World Materials Congress Award of ASM International (1988), the Gaede-Langmuir Award of the American Vacuum Society (1988), and the Industrial Research Institute Achievement Award of the Industrial Research Institute, Inc. (1988). He is a Fellow of the American Physical Society, and the American Academy or Arts and Sciences. He is a member of the American Vacuum Society, the Electrochemical Society, the Materials Research Society, the National Academy of Engineering, and the National Academy of Sciences.

*

Deborah L. Sivco, photograph and biography not available at the time of publication.